AFRL-SN-WP-TR-1999-1104

ALL-SOLID-STATE TUNABLE (Cr^{2+}) LASER

KENNETH L. SCHEPLER
JASON McKAY

SENSORS DIRECTORATE
AIR FORCE RESEARCH LABORATORY
AIR FORCE MATERIEL COMMAND
WRIGHT-PATTERSON AFB, OH 45433-7318

JULY 1999

FINAL REPORT FOR 02/20/1997 – 05/31/1999

SENSORS DIRECTORATE
AIR FORCE RESEARCH LABORATORY
AIR FORCE MATERIEL COMMAND
WRIGHT-PATTERSON AIR FORCE BASE OH 45433-7318

NOTICE

USING GOVERNMENT DRAWINGS, SPECIFICATIONS, OR OTHER DATA INCLUDED IN THIS DOCUMENT FOR ANY PURPOSE OTHER THAN GOVERNMENT PROCUREMENT DOES NOT IN ANY WAY OBLIGATE THE US GOVERNMENT. THE FACT THAT THE GOVERNMENT FORMULATED OR SUPPLIED THE DRAWINGS, SPECIFICATIONS, OR OTHER DATA DOES NOT LICENSE THE HOLDER OR ANY OTHER PERSON OR CORPORATION; OR CONVEY ANY RIGHTS OR PERMISSION TO MANUFACTURE, USE, OR SELL ANY PATENTED INVENTION THAT MAY RELATE TO THEM.

THIS REPORT IS RELEASABLE TO THE NATIONAL TECHNICAL INFORMATION SERVICE (NTIS). AT NTIS, IT WILL BE AVAILABLE TO THE GENERAL PUBLIC, INCLUDING FOREIGN NATIONS.

THIS TECHNICAL REPORT HAS BEEN REVIEWED AND IS APPROVED FOR PUBLICATION.

Kenneth L. Schepler, PhD
Principal Scientist
EO Targeting Branch

Henry Lapp, Chief
EO Targeting Branch
EO Sensor Technology Div

STEVEN R. PETERSEN, Colonel, USAF
Chief, EO Sensor Technology Div
Sensors Directorate

Do not return copies of this report unless contractual obligations or notice on a specific document require its return.

REPORT DOCUMENTATION PAGE	Form Approved OMB No. 0704-0188

1. AGENCY USE ONLY *(Leave blank)*	2. REPORT DATE	3. REPORT TYPE AND DATES COVERED
	JULY 1999	FINAL REPORT FOR 02/20/1997 - 05/31/1999

4. TITLE AND SUBTITLE
ALL-SOLID-STATE TUNABLE (Cr2+) LASER

5. FUNDING NUMBERS
IN-HOUSE
PE 61102
PR 2301
TA AA
WU 03

6. AUTHOR(S)
KENNETH L. SCHEPLER
JASON McKAY

7. PERFORMING ORGANIZATION NAME(S) AND ADDRESS(ES)
SENSORS DIRECTORATE
AIR FORCE RESEARCH LABORATORY
AIR FORCE MATERIEL COMMAND
WRIGHT-PATTERSON AFB, OH 45433-7318

8. PERFORMING ORGANIZATION REPORT NUMBER

9. SPONSORING/MONITORING AGENCY NAME(S) AND ADDRESS(ES)
SENSORS DIRECTORATE
AIR FORCE RESEARCH LABORATORY
AIR FORCE MATERIEL COMMAND
WRIGHT-PATTERSON AFB, OH 45433-7318
POC: KENNETH L. SCHEPLER, AFRL/SNJT, 937-255-3804 EXT 312

10. SPONSORING/MONITORING AGENCY REPORT NUMBER
AFRL-SN-WP-TR-1999-1104

11. SUPPLEMENTARY NOTES

12a. DISTRIBUTION AVAILABILITY STATEMENT
APPROVED FOR PUBLIC RELEASE, DISTRIBUTION UNLIMITED

12b. DISTRIBUTION CODE

13. ABSTRACT *(Maximum 200 words)*

We investigated the spectroscopy and laser performance of Cr2+ ions doped into II-VI semiconductors. Cr2+ ions in CdSe exhibited strong broadband absorption in the 1.5-2.4 micron band peaked at 1.9 microns. Broadband fluorescence was present in the 1.8-2.8 micron region with a 6 microsecond lifetime in the 60-300 K temperature range. We demonstrated pulsed lasing of Cr2+:CdSe using a 1 kHz, Q-switched, 2.05-micron, Tm,Ho:YLF pump laser. The Cr2+:CdSe laser produced 500 mW of broadband output centered at 2.6 microns with 48% absorbed power conversion efficiency. With a larger pump beam to prevent coating damage, 815 mW was demonstrated. Tuning over the 2.3-2.9 micron range was demonstrated using a grating as the tuning element with 350 mW average power at the peak of the tuning curve.

14. SUBJECT TERMS	15. NUMBER OF PAGES
lasers, infrared, chromium, tunable	27
	16. PRICE CODE

17. SECURITY CLASSIFICATION OF REPORT	18. SECURITY CLASSIFICATION OF THIS PAGE	19. SECURITY CLASSIFICATION OF ABSTRACT	20. LIMITATION OF ABSTRACT
UNCLASSIFIED	UNCLASSIFIED	UNCLASSIFIED	SAR

TABLE OF CONTENTS

LIST OF FIGURES

LIST OF TABLES

ACKNOWLEDGEMENTS

We gratefully acknowledge the efforts of Lee Shiozawa and Gary Catella of Cleveland Crystals, Inc. who grew and fabricated the crystals used in this effort. We also acknowledge their technical assistance with data interpretation. Finally, we wish to thank the Sensors Directorate and AFOSR for funding support of this Entrepreneurial Research effort.

1. INTRODUCTION

This technical report briefly summarizes the research performed to investigate and demonstrate laser performance of Cr^{2+}-doped cadmium selenide (CdSe). Cr^{2+} lasers have the potential of high average output power, broadband infrared (IR) tunability, room temperature operation, and completely solid-state operation. Such lasers could be efficient IR sources for infrared missile countermeasures, eyesafe laser radar, target identification, and chemical sensing. Commercial uses in spectroscopy and environmental sensing are also of interest.

There are several ways to realize a laser source in the mid-IR such as semiconductor lasers, chemical lasers, and nonlinear frequency conversion of shorter (e.g. Nd lasers) or longer (e.g. CO_2 lasers) wavelengths to the mid-IR region. But these sources have limitations such as complexity, low power, or cryogenic operation that make them impractical for many uses. Recently, Cr^{2+} transition metal ions have shown the potential to be simple, efficient, tunable sources in the mid-infrared. Efficient room temperature lasing was first demonstrated with Cr^{2+} active ions doped into II-VI crystalline chalcogenide hosts such as ZnSe and ZnS.[1,2] Concurrently with our investigations of Cr^{2+}:CdSe, Cr^{2+}:CdMnTe[3] was also demonstrated to be an efficient laser material.

But CdSe has some important advantages. CdSe is easily grown in large sizes with excellent single-crystal quality. Cr^{2+} ions are easily diffused into CdSe making doping straightforward. Thus laser crystals are readily available and are relatively inexpensive. Room-temperature Cr^{2+} radiative emission efficiency is near 100% meaning that nonradiative loss is not a factor in laser operation. Finally, the CdSe crystal is uniaxially

birefringent. This means that laser emission is automatically polarized. Also, CdSe does not have inversion symmetry making it capable of nonlinear interactions simultaneous with laser action.

2. SPECTROSCOPY

Like ZnSe, CdSe is a II-VI semiconductor crystal with 6mm point group symmetry. The small phonon frequencies of II-VI materials when compared to oxides should make nonradiative relaxation rates for dopant ions small even at room temperature. Also, large absorption and emission cross-sections between the Cr^{2+} crystal-field-split $^5T_2$ ground state and the first excited ^5E state are expected since the transitions are spin allowed. Substitution of Cr^{2+} ions into the CdSe lattice is expected based on consideration of ionic radii [Cd^{2+} (.95Å), Cr^{2+} (.82Å)] in six-fold coordination.

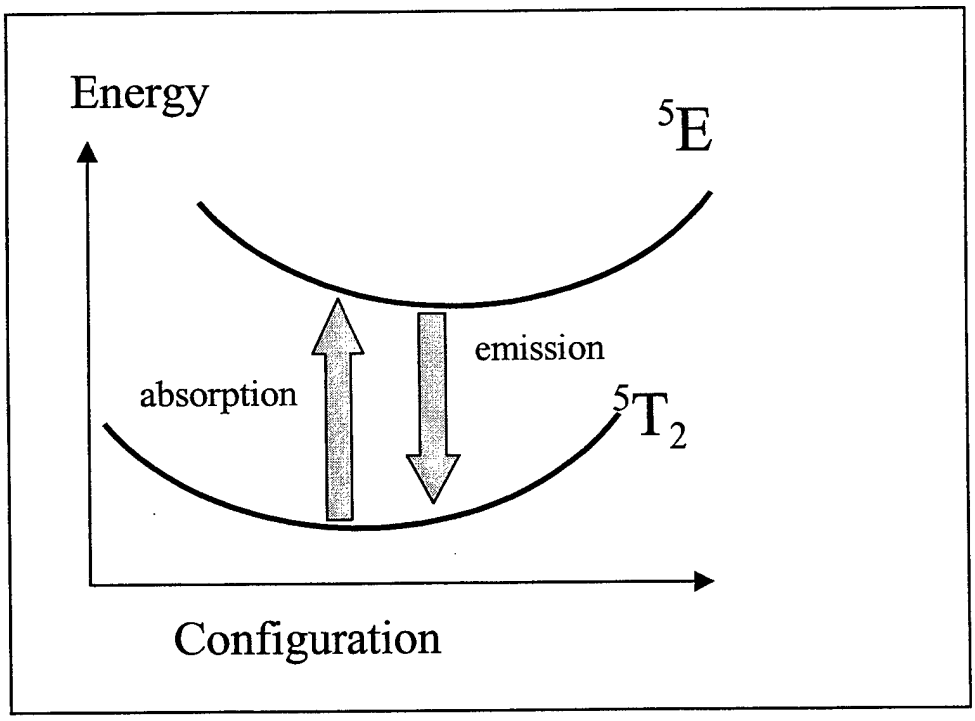

Figure 1. Configuration coordinate diagram for Cr^{2+} ions. The up arrow represents absorption and the down arrow represents fluorescence.

The first Cr:CdSe investigated spectroscopically[4] was grown by vapor transport with 0.5 wt% CrSe in the charge. A large, single crystal, 8 mm x 8 mm x 11 mm, was fabricated from the boule. A second boule solidified directly from the melted charge, but it was polycrystalline and cracked due to anisotropic thermal expansion of CdSe. Electron microprobe measurements of chromium abundance showed that 400 ppm (±200 ppm) Cr was in the polycrystalline material. Chromium levels were too small to measure directly in the single crystal.

Transmission measurements of the single crystal at room-temperature showed a broadband absorption feature peaked at 1.9 μm which corresponds to the spin-allowed ^5E to $^5T_2$ transition of Cr^{2+} ions; this spectrum is shown in Figure 2. Absorption coefficients at the 1.9-μm peak were measured for the single crystal and a 300-μm thick wafer of the polycrystalline material to calculate Cr^{2+} concentration in the single crystal. The single crystal Cr^{2+} concentration was 4 ppm (± 3 ppm) indicating that very little chromium was transported to the vapor-grown crystal. Based on this indirectly measured chromium concentration and the CdSe density of 5.81 g/cm^3, the absorption cross section peak, $\sigma_{abs,}$ was estimated to be 3 x 10^{-18} cm^2.

When pumping at 1.9 μm, broadband emission was observed over the 1.8-2.8 μm region as shown by the right-hand trace in Figure 2. Qualitative measurements with a more sensitive detector showed emission out to 3200 nm. The emission peak is Stokes shifted only 300 nm relative to the absorption peak by the crystal field. Thus, there is significant overlap which reduces the potential lasing range to regions where the emission cross-section is larger than the absorption cross-section, i.e. laser wavelengths > 2200 nm.

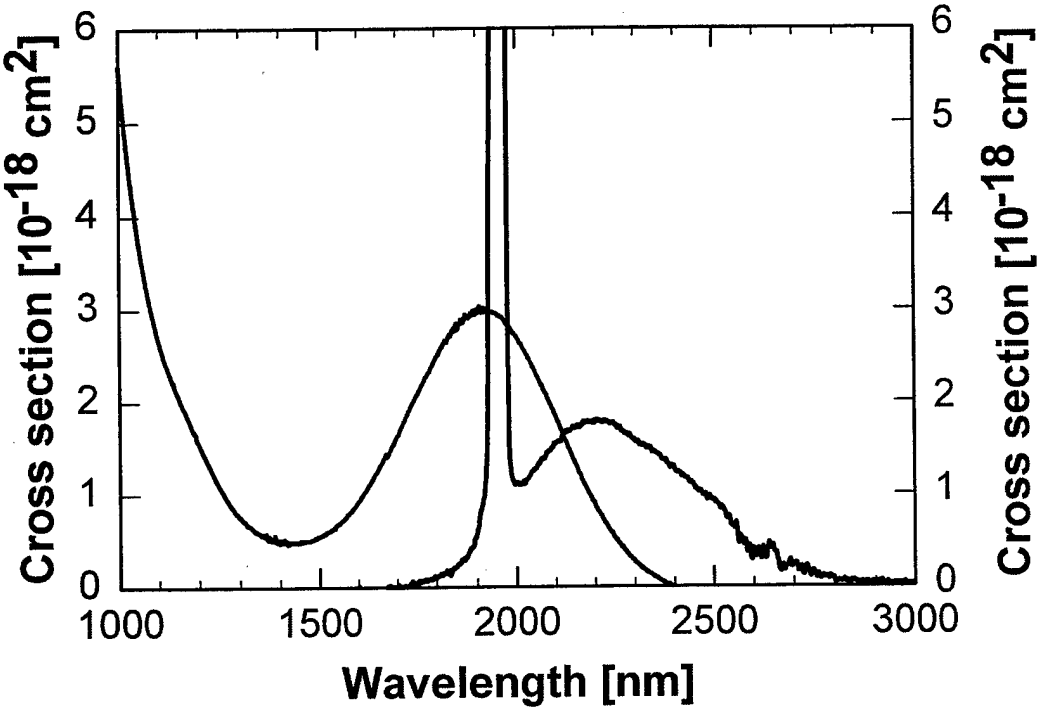

Figure 2. Cr^{2+}:CdSe room temperature absorption and emission spectra.

We measured fluorescence lifetime as a function of temperature using an acousto-optically modulated Ti: sapphire laser beam operating at 755 nm. Pumping at 755 nm also produced strong emission in the same infrared region. As shown in Figure 3, emission lifetime was constant throughout the 60-300 K temperature range with a value of 6 μs. This implies that Cr^{2+} nonradiative relaxation is negligible and quantum efficiency of the radiative relaxation is near unity even at room temperature. An emission cross-section, σ_{emis} was calculated using the Einstein relation to be 1.8 x 10^{-18} cm^2. Cr^2:CdSe lifetime is shorter (6 μs versus 8 μs) and absorption emission cross-sections are larger by factors of 3 and 2, respectively, than those measured by DeLoach et al.[1] for Cr^2 :

ZnSe. Table 1 summarizes the relative properties.

Table 1 Cr^{2+} Spectroscopic Properties in CdSe and ZnSe

Property	CdSe	ZnSe
Cr^{2+} concentration (ppm)	4	44
absorption cross-section (10^{-18} cm^2)	3	0.87
emission cross-section (10^{-18} cm^2)	1.8	0.92
lifetime (μsec)	6	8

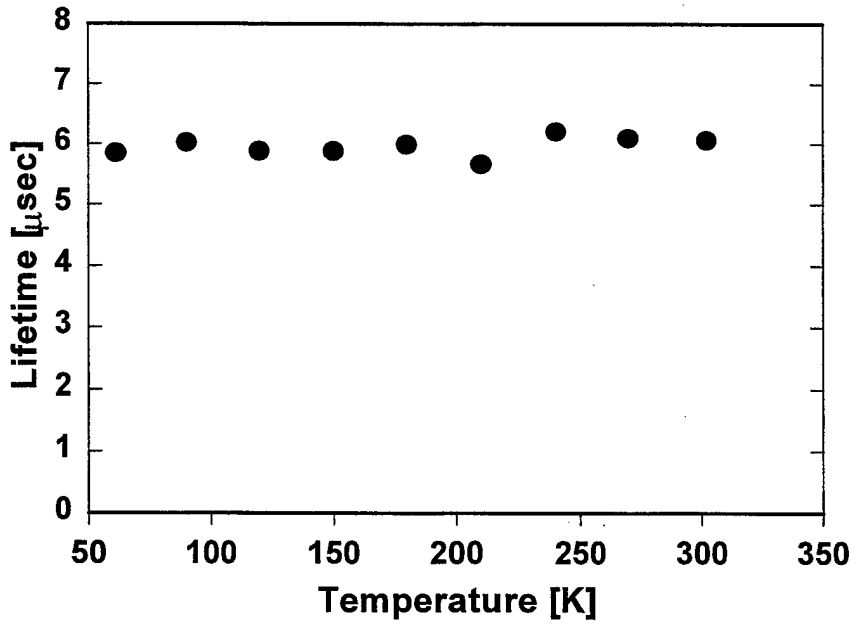

Figure 3. Fluorescence of Cr^{2+} ions is independent of temperature indicating that nonradiative relaxation is not significant.

3. LASER OPERATION

Our first demonstration of Cr^{2+}:CdSe lasing used a vapor-grown sample of Cr^{2+}:CdSe pumped at 2.09 μm with a flashlamp-pumped, Q-switched, Cr,Tm,Ho:YAG laser. The Cr^{2+}:CdSe laser achieved a 58% (output)/(absorbed) energy slope efficiency[5]. However, the sample had very low chromium concentration (~4 ppm) and uncoated, high Fresnel reflectivity surfaces that resulted in an overall optical-to-optical efficiency of only 5%.

3.1 Pump Laser

Since the Cr,Tm,Ho:YAG laser was only capable of operating at low repetition rates, we assembled a diode-pumped Tm,Ho:YLF laser that was capable of both high repetition rate Q-switched operation and cw operation for further Cr^{2+}:CdSe laser testing. This Tm,Ho:YLF laser was diode pumped by a fiber-coupled Opto-Power 15-W cw diode array operating at 792 nm. The laser crystal was cryogenically cooled in a dewar. An AO modulator provided high repetition rate Q-switched operation at 2.05 μm. The Tm,Ho:YLF laser had high flexibility in output pulse-width and repetition rate, running from 500-Hz, 50-ns pulses to cw. The laser oscillator produced 6 W of continuous or Q-switched output power at 2.05 μm.

For the high-power pumping experiments reported below, we ran the Tm,Ho:YLF laser (and thus the chromium laser) Q-switched at repetition rates of 1, 2, 5, and 10 kHz. For the initial demonstration, the Tm,Ho:YLF oscillator was operated Q-switched at 2.5

mJ/pulse at 1 kHz. The laser pulses were 200 ns FWHM and pulse amplitude stability was on the order of 10-15%. A diagram of the setup is shown below in Figure 4.

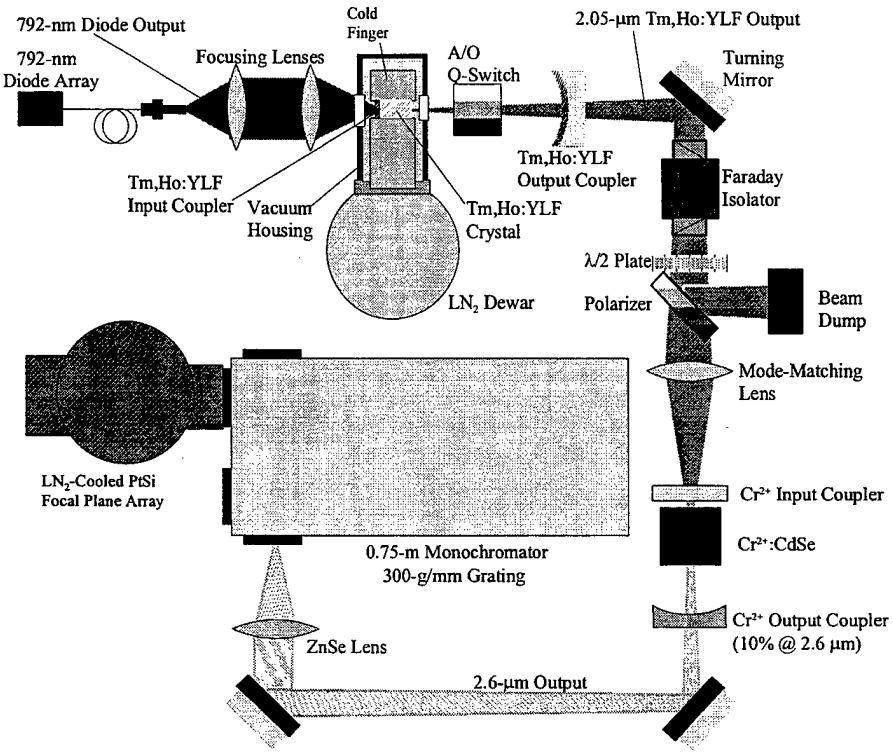

Figure 4. Schematic of the Cr^{2+}:CdSe laser experimental setup.

To keep the pump laser running efficiently, we left the diode current (and cooling water temperature) at a constant setting and used a half-wave plate and polarizer to provide attenuation of the 2.05-μm input to the chromium resonator. An isolator in the system was required, as feedback from the chromium laser output mirrors caused unstable behavior in the 2.05-μm pump laser. A 25-cm lens focused the 2.05-μm pump beam down to a 0.6-mm diameter inside the Cr^{2+}:CdSe crystal, providing pulsed fluence levels up to 0.6 J/cm^2.

3.2 Cr^{2+} Laser Resonator

The Cr^{2+}:CdSe crystals used in our laser experiments were also grown by Cleveland Crystals, Inc. The crystals were grown as pure CdSe and then chromium was diffused into CdSe slabs at elevated temperatures. Two laser crystals were fabricated, one 7-mm long piece with nominal 50-ppm Cr^{2+} concentration and one 10-mm long piece with nominal 15-ppm Cr^{2+} concentration. The crystals were coated to be anti-reflective (AR) at 2 μm and broadband AR centered at 2.5 μm. Measurements using the 2.05-μm laser showed that the coatings had a reflectivity of 7%/surface at 2.05 μm (compared to 17%/surface for uncoated CdSe). The 10-mm crystal absorbed 43% of the incident 2.05-μm power in a single pass; the 7-mm crystal absorbed 57%. The Cr^{2+}:CdSe crystals were placed in a 4-cm hemispherical cavity with 10% output coupling at 2.5 μm. The resonator increased the 2.05-μm absorption to 57% and 63% for the 10-mm and 7-mm crystals respectively, due to a 64% reflectivity at 2.05 μm by the output coupler.

The chromium absorption started to saturate due to depletion of the ground state population at input pulse energy densities of 0.1 J/cm^2 to 0.3 J/cm^2 when the crystal was not lasing. When lasing, however, the crystal absorption was close to its small-signal value. Up to a 33% difference was seen in the high-chromium concentration sample when comparing pump absorption during lasing to the absorption when the cavity was misaligned. For this reason we will report laser performance in terms of absorbed pump power rather than incident pump power.

FTIR measurements showed both Cr^{2+}-doped crystals had 90% transmission at 2.6 μm. Direct laser transmission and reflection measurements of the samples showed 1%

reflection/surface at 2.6 μm, and 92% transmission at 2.6 μm. Therefore, there is significant loss occurring inside the crystals. Likely mechanisms for this loss include bulk Cr:CdSe scattering, Cr^{2+} absorption on the wing of the 1.9-μm absorption peak, and coating absorption.

3.3 Initial High Power Cr^{2+}:CdSe Laser Demonstration

The initial high power, high repetition rate, Cr^{2+}:CdSe laser performance[6] is shown in Figure 5. The crystals had thresholds in the 20-40 μJ range and produced up to 230 mW of average power output in bursts of several 50- to 100-ns pulses per 200-ns pump pulse.

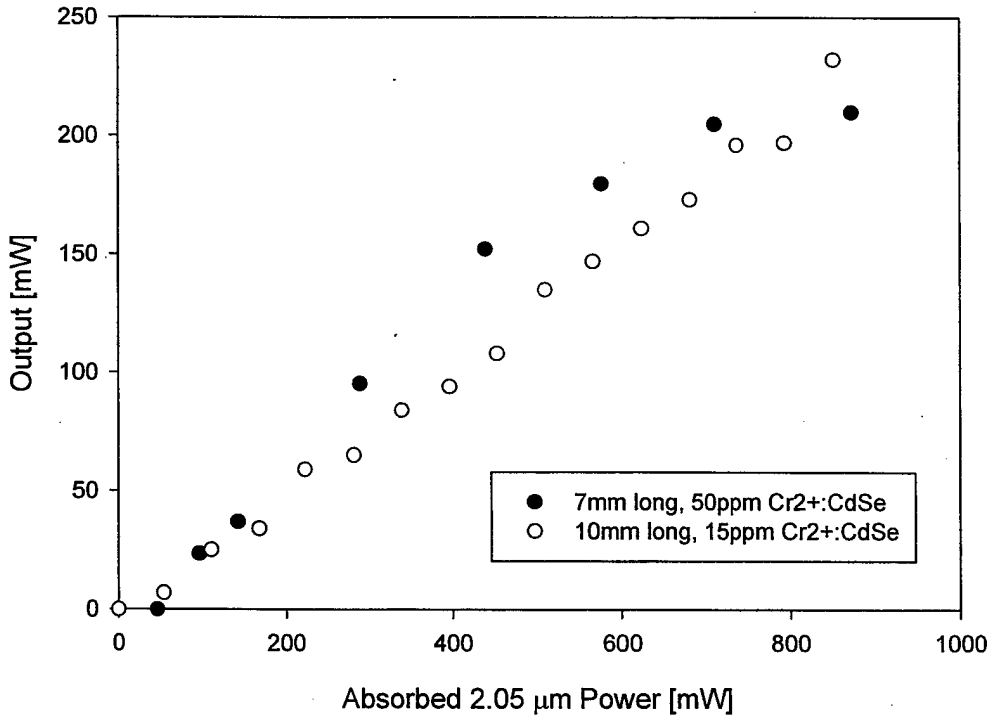

Figure 5. Initial 1 kHz high power laser operation (0.3 mm pump radius).

With the increase in pump power or precision of the cavity alignment, the number of output pulses increased and the length of each pulse decreased, to the point where our

experiment could not distinguish the separate pulses anymore. At that point, the output pulse width was on the order of 200 nsec. Beam quality was good, with M^2 values of 2.2 in the horizontal and vertical axes. The beam quality changed dramatically with small changes in cavity length, but efficiency did not, indicating that the laser would readily operate multi-mode if given the chance. The 7-mm sample had an initial slope efficiency of 38.5%, but it decreased rapidly after incident pump power reached the 800-mW level, resulting in an optical conversion efficiency of 24% at 210-mW output. Thermal lensing, and perhaps slow coating damage, are likely candidates for the degradation in efficiency. The 10-mm crystal had a 27% slope efficiency from the start, but it did not diminish with increase in pump power. Average output power of 230 mW was achieved with an optical conversion efficiency of 27%. Both crystals produced output polarized along the a-axis, and did not exhibit sensitivity to the polarization of the pump laser. Overall output efficiency vs. input power incident on the crystal for both crystals was 13-15% (only 60% of the pump was absorbed in the crystals). The overall efficiency and maximum pulse energy are a factor of three higher than what we achieved in the 4 ppm crystal primarily due to higher chromium concentrations and coated surfaces.

The chromium laser bandwidth was measured using a 1-inch, 1024-element, LN_2-cooled PtSi focal plane array detector mounted on the exit port of a 0.75-m monochromator. Each pixel in the array spanned 0.092 nm using a 300-groove/mm grating, and the overall field of view was 94 nm. The PtSi output voltage was averaged for 250 sweeps on the oscilloscope, then bias corrected and imported to a computer. Both crystals exhibited similar bandwidths, operating over a range from 2.56 μm to 2.73 μm

with 75-nm FWHM. This wavelength range overlaps a strong water absorption band in the atmosphere, so the emission spectrum was heavily structured.

3.4 Damage

Damage measurements conducted with the 2.05-μm laser indicated that uncoated Cr^{2+}:CdSe crystals had 1-kHz pulsed damage thresholds on the order of 1 J/cm^2. However, the coatings on the laser crystals failed at an input of 0.6 J/cm^2. While lasing, the crystals showed still lower damage thresholds, energy density levels closer to 0.3 J/cm^2. Damage took several minutes to become noticeable, and was difficult to see with the naked eye, looking like a faint spot on the coatings, making the determination of exact damage threshold difficult. Microscopic examination showed small bubbles or melted spots on the coatings, distributed throughout the area of beam contact on both faces of the crystal. For the most part, large scale "drilling" or pitting (common signs of damage due to pulse energy) were not seen on Cr^{2+}:CdSe at this power level, even at scratches or places where the coatings had damaged.

3.5 Power Scaling

After the initial demonstration, the system was reconfigured for higher average power operation. An amplifier stage was added to the Tm,Ho:YLF pump laser to provide up to 6.5 watts of 2.05-μm pump power incident on the crystals. As a bonus, the Faraday isolator was no longer required because new optics which do not reflect highly at the pump wavelength were used. Also, the optical path between the 2-μm oscillator and the

2.6-μm resonator became much longer. The Cr^{2+} resonator configuration was the same: a hemispherical short cavity with a high reflecting input mirror and a partially reflecting output mirror. Cavity lengths of 8-16 cm were used.

Two experiments were conducted: one at 2 watts and one at 6.5 watts of pump power incident on the crystals. To avoid further damage to the samples, the maximum pump energy density was kept at or below 0.3 J/cm^2. The 2-watt experiment used a pump beam radius of 0.45 mm (0.31 J/cm^2) and the 6.5-watt experiment used an effective pump beam radius of 1.2 mm (0.14 J/cm^2). The 2-watt experiment was conducted with only the oscillator in the system. The amplifier was added for the 6.5 -watt experiment, as we had only about 4 watts usable after optics losses from the oscillator alone. However, the amplifier also acted as a cylindrical lens, transforming the round oscillator output into an elliptical beam with an ellipticity of 1.5:1. Thus, the high power experiment was pumped by an elliptical beam with semiaxes of 1.5 mm and 1 mm.

The Cr^{2+} resonator in the 2-watt experiment was a simple three-element cavity consisting of a flat input coupler, the crystal, and a concave partially reflective output coupler. We used the 50-ppm Cr^{2+} crystal in this experiment. As mentioned, the pump beam radius at the crystal was 0.45 mm. The mirror separation was 8 cm. The input coupler was a flat CaF_2 mirror with 95% transmission at 2 μm and 98% reflection at 2.6 μm. Two different output couplers, identical except for 2.6-μm reflectivity, were used in the experiment. Both were plano-concave CaF_2 mirrors with about 30% reflectivity at 2 μm, and 20-cm radius of curvature. One had a 2.6-μm reflectivity of 50%; the other had a 2.6-μm reflectivity of 75%. For both output couplers, 500 mW of 2.6-μm output was demonstrated (see Figure 6a). The threshold was 40 mW (absorbed power) with the 75%

reflector in the resonator, and the absorbed power slope efficiency was 39%. With the 50% reflector, the threshold was 65 mW and the slope efficiency was 48%. Since about 60% of the incident pump power was absorbed in the crystal, we achieved an overall

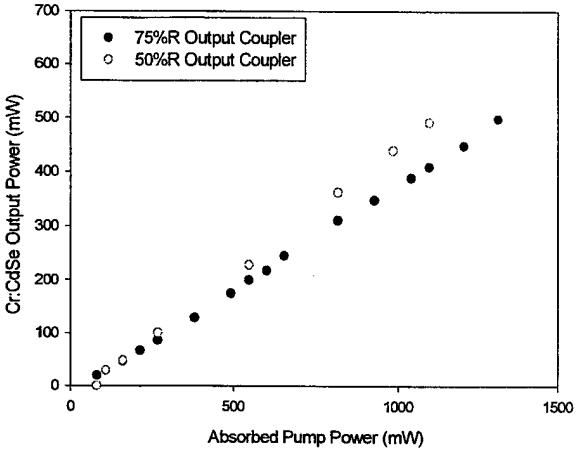

Figure 6a: 2-W Exp. (0.45 mm pump radius)

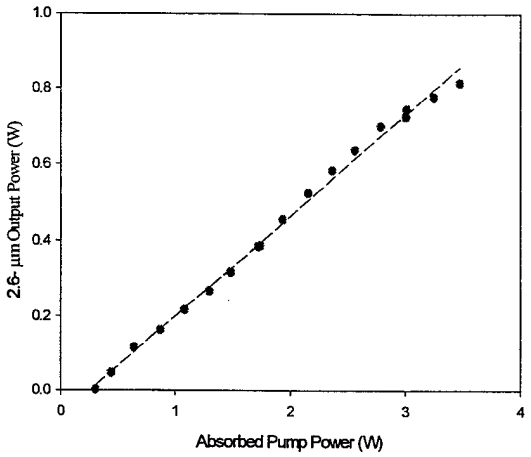

Figure 6b: 6.5-W Exp. (1,1.5 mm pump semiaxes)

optical input-output efficiency of 28% with the 50% output coupler.

The 6.5-watt experiment used a hemispherical resonator configuration with a cavity length of 16 cm and a 50% output coupler with a 100-cm radius of curvature. Due to an asymmetric thermal lens in the amplifier, the pump beam came to an elliptical focus with a 3-mm major axis and a 2-mm minor axis at the crystal. We saw up to 815 mW of output power at 2.6 µm (see Figure 6b). However, we did not achieve the high efficiency of the 2-watt experiment. The absorbed power threshold was 250 mW and the absorbed power conversion efficiency was 27%. This resulted in an input-output efficiency of 16%, comparable to that of our initial demonstration with the 90% R output mirrors. Possible reasons for the efficiency loss are mode-matching problems with the elliptical beam in the hemispherical resonator, and the unfortunate difficulty of finding a large enough undamaged area on the crystal "sweet spot" to allow 50% efficiency. The results

indicate that it should be possible to develop a 1 to 2 watt broadband, pulsed (1 kHz) source at 2.6 μm using Cr^{2+}:CdSe, with only minor improvements to this experiment, such as improved mode matching and an undamaged crystal.

The amplitude stability of the 2.6-μm output in the power scaling experiment was very good. Pulse to pulse variations of 5%-10% were seen, and average power varied about 2-3% over the course of 10 minutes, much of which was correlated to power fluctuations in the pump laser. Alignment did not drift over the course of the experiment (1 hour), and cooling was not required. This is good evidence that we had not yet reached the coating damage intensity, as that regime is characterized by rapid output power fluctuations of up to 15%, along with a non-recoverable gradual decrease in the overall output power over the course of 10-30 minutes. In fact, we have found that the best way to detect the onset of coating damage is to look at the short-term amplitude variation of the output beam. With the pump laser constant, 2.6-μm power oscillations of 5% or more over the course of 1-20 seconds indicates likelihood of damage being done.

3.6 Thermal Effects

Cadmium selenide has a thermal conductivity[7] of about 65 mW/cm-K, only a factor of four larger than that of fused silica. Accordingly, we expected to encounter thermal effects requiring compensation and/or significant cooling. However, we did not encounter any significant thermal effects (lensing or temperature-dependent lasing efficiency) at the 1 kHz repetition rate. We did observe thermal lensing occurring at pulse repetition rates faster than 1 kHz. The lensing became much worse as the repetition

rate of the pump laser was increased, keeping power constant. The pump power that slightly degraded lasing efficiency at 2 kHz completely destabilized the 4-cm cavity at 10 kHz. The thermal lens could be detected by the diameter of the transmitted of the pump beam at a distance of ~25 cm past the chromium laser output coupler. At 1 kHz, the beam had a 2-mm diameter at this point. At 10 kHz, the beam had a diameter of over 1 cm. The transmitted beam enlarged only slightly more going from 10 kHz to cw operation. The dependence of the thermal lens on pulse repetition rate, chromium concentration, average power density, and cooling has not yet been completely investigated. Thermal lensing appears likely to be a major issue in the demonstration of a high power, cw device. However, thermal lensing can be ignored at repetition rates equal to or lower than 1 kHz.

4. WAVELENGTH TUNING

The very broadband emission should make Cr^{2+} lasers capable of tunable lasing. We have investigated wavelength selection using a YLF birefringent filter, a prism, and a diffraction grating. The YLF single-thickness birefringent filter provided tuning but did not significantly reduce the bandwidth so we will not discuss it further.

4.1 Prism Tuning

The experimental setup for prism tuning is shown in Figure 7. The pump laser was the same as described above. In the wavelength tuning experiment, the Cr^{2+}:CdSe crystal was placed near the flat input coupler of a 14-cm long hemispherical cavity; the input coupler was highly reflective in the 2.3-3 μm region and 90% transmissive at the 2.05-μm pump wavelength. The 30-cm radius of curvature output coupler had 10-30% output coupling in the 2.3-2.9 μm spectral region with a parabolic transmission minimum centered at 2.4 μm. Wavelength tuning was achieved using a sapphire prism placed 3 cm from the output coupler. The chromium laser output was directed through an uncoated ZnSe lens into a 0.75-m monochromator with a 1-5 μm PtSi focal plane array for wavelength measurements.

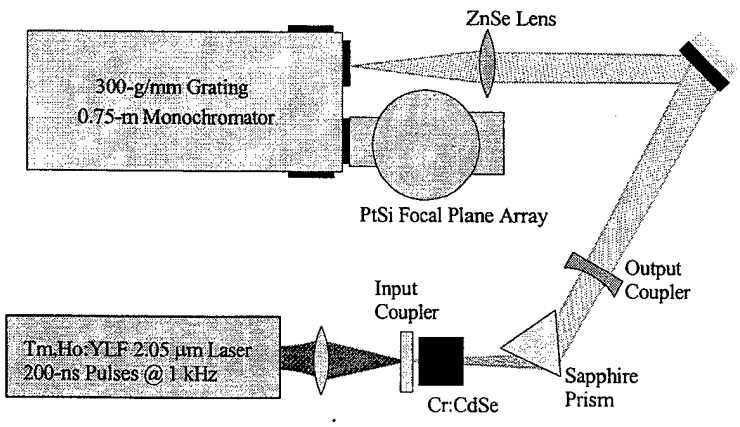

Figure 7: Schematic of the tunable Cr^{2+}:CdSe laser experimental setup.

With incorporation of a sapphire prism in the lengthened resonator for wavelength discrimination, we observed continuous wavelength tuning over the entire 2.3-2.9 μm spectral region. With an average pump power of 840 mW, 360 mW absorbed, up to 62 mW of tunable output was generated as shown in Figure 8. Bandwidth was typically ~15 nm, but this could easily be narrowed by lengthening the resonator. The tuning limits were primarily set by the high reflectivity range of the input coupler and not by the Cr^{2+} emission spectrum.

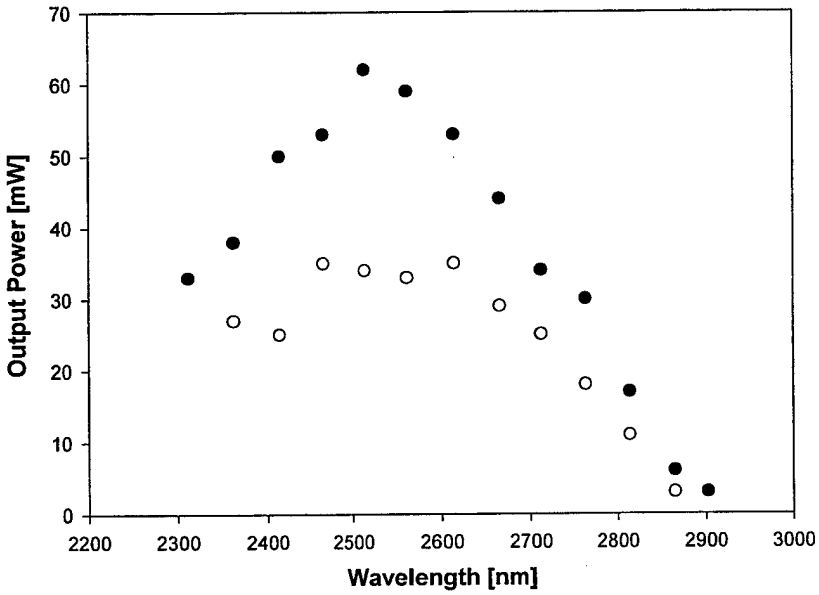

Figure 8. Cr^{2+}:CdSe laser tuning. ● = output power with 840 mW incident pump power, ○ = output power with 420 mW incident pump power.

4.2 Grating Tuning

Our best tuning results were achieved with a 295 groove/mm diffraction grating blazed at 2.6 μm. The diffraction grating tuning schematic is shown in Figure 9. We used a three mirror folded resonator to prevent the pump light from reaching the diffraction grating. The length of each resonator leg was 60 cm. The folding mirror/input coupler was a 100-cmcc, broadband 2.3-3 μm high reflector that passed 90% of the pump light for input coupling. An identical mirror was used on the other end of the pumped leg of the cavity to dump the remaining pump light. The diffraction grating was used as the third mirror in the folded cavity, with the first-order diffracted beam providing the resonator feedback. The specular reflection from the grating was the output beam. The

effective output coupling was 20% at 2.6 μm, rendering the laser somewhat under-coupled.

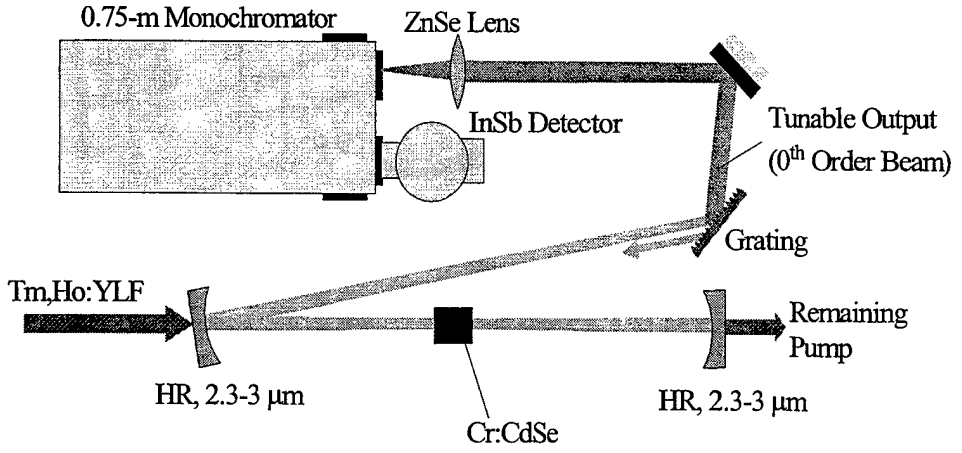

Figure 9. Schematic of the grating-tuned Cr^{2+}:CdSe laser configuration.

The diffraction grating produced tuning from 2.3 to 2.9 μm and narrowed the bandwidth to 10 nm FWHM. The tuning curve is shown in Figure 10. Up to 350 mW of average power was demonstrated at 2.5 μm, with an absorbed power efficiency of 22%. The output power fell off gradually to 50 mW at 2.32 μm and 2.88 μm, providing nearly 600 nm of tunability. Decreased output power accompanied by a clearly audible 1-kHz tone coming from the laser resonator was noted at certain wavelengths where there was significant overlap with the atmospheric water absorption lines in the 2.6-2.8 μm region. The tuning range appears to be limited by the AR coatings on the long wavelength end and ground state absorption on the short wavelength end. It may be possible to increase the tuning range towards longer wavelengths by using broader bandwidth AR coatings or Brewster surfaces on the crystal to reduce the long wavelength resonator losses.

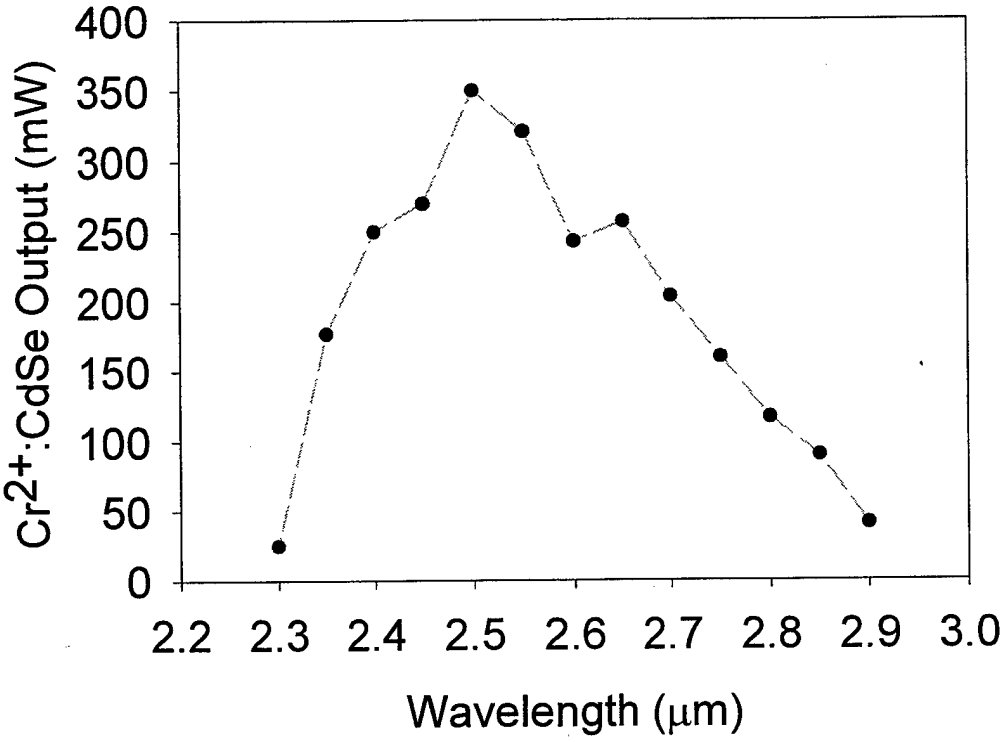

Figure 10. Cr^{2+}:CdSe wavelength tuning using a diffraction grating. Bandwidth was 10 nm throughout the tuning range.

5. CONCLUSION

In summary, Cr^{2+}:CdSe has been demonstrated to be a promising new mid-IR laser material. At 1 kHz repetition rate, we achieved an average power of 500 mW at 2.6 μm with 48% conversion efficiency of absorbed power with room-temperature operation. We achieved up to 815 mW using a larger pump but with a reduced efficiency of 27%. The beam quality of the initial 230-mW resonator was good, with an M^2 of 2.2 in both the horizontal and vertical directions. Beam quality of the higher power demonstrations has not yet been measured, though it appears to be similar. The optical quality of these first crystals is quite good, and we expect improvement as we optimize the growth and fabrication techniques.

We also demonstrated high-power broad tunability of Cr^{2+}:CdSe using a diffraction grating as an output coupler. The laser had tunability from 2.3-2.9 μm with 10-nm bandwidth and up to 350 mW average power output.

The obstacles in the way of scaling to higher powers and eventual cw operation appear to be chromium-induced crystal loss, low coating damage thresholds, and thermal lensing. The prospects of Cr^{2+}:CdSe becoming a viable source of high power, tunable radiation in the 2.5-2.8-μm range look very promising.

6. REFERENCES

1 L. D. DeLoach, R. H. Page, G. D. Wilke, S. A. Payne, and W. F. Krupke, *IEEE J. Quantum Electron.* **32,** 885-895 (1996).

2 R. H. Page, K. I. Schaffers, L. D. DeLoach, G. D. Wilke, F. D. Patel, J. B. Tassano, S. A. Payne, W. F. Krupke, K.-T. Chen, and A. Burger, *IEEE J. Quantum Electron.* **33,** 609-619 (1997).

3 U. Hömmerich, X. Wu, V. R. Davis, S. B. Trivedi, K. Grasza, R. J. Chen, and S. Kutcher, *Opt. Lett.* **22,** 1180-1182 (1997).

4 K. L. Schepler, S. Kück, and L. Shiozawa, *J. Lumin.* **72-74,** 116-117 (1997).

5 J. McKay, K. L. Schepler, and S. Kück, in *1998 OSA Annual Meeting*, Vol. paper THGG1 (Optical Society of America, Washington DC, Baltimore MD, 1998), pp. 136.

6 J. McKay, K. L. Schepler, and G. Catella, in *Advanced Solid State Lasers*, TOPS Volume 26, edited by M. M. Fejer, H. Injejay, and U. Keller (Optical Society of America, Washington DC, Baltimore MD, 1999), pp. 420-426.

7 J. D. Beasley, *Appl. Opt.* **33** (1994).